Serb. Astron. J. № 206 (2023), 39 - 45
DOI: https://doi.org/10.2298/SAJ2306039Z

UDC 52–121 + 52–732 + 52–77
Preliminary report

A SEARCH FOR FAST RADIO BURSTS ASSOCIATED WITH GAMMA-RAY BURSTS USING THE YNAO 40-M RADIO TELESCOPE

Y. F. Zhang[1,2], Z. G. Wen[2], N. Wang[2], L. F. Hao[3], J. P. Yuan[2], R. Yuen[2], X. F. Duan[2,4] and Z. Wang[1,2]

[1] *School of Physical Science and Technology, Xinjiang University, Urumqi, Xinjiang, 830046, People's Republic of China*

[2] *Xinjiang Astronomical Observatory, Chinese Academy of Sciences, 150, Science-1 Street, Urumqi, Xinjiang, 830011, People's Republic of China*

[3] *Yunnan Astronomical Observatory, Chinese Academy of Sciences, Kunming, 650011, People's Republic of China*

[4] *Xinjiang Key Laboratory of Microwave Technology, Urumqi, Xinjiang, 830011, People's Republic of China*

E–mail: *wenzhigang@xao.ac.cn*

(Received: April 24, 2022; Accepted: March 31, 2023)

SUMMARY: We report on the search results of Fast Radio Bursts (FRBs) from three Gamma-ray Bursts (GRBs) at 2256 MHz using the 40-m radio telescope located at the YunNan Astronomical Observatory (YNAO). The search for signals was triggered by the Burst Alert Telescope (BAT) onboard the Swift satellite. Radio single pulses are searched in the data over a large range of dispersion measure from 0 to 5000 pc/cm^3 in step of 50 pc/cm^3. No FRB-like emission from the prompt phase of GRBs are detected with significance $> 5\sigma$. If there are FRBs related to the GRBs, we set an upper limit on the flux density of radio pulses of 2.5 Jy for GRB140512A and 8.0 Jy for GRBs 140629A and 140703A with the sensitivity of the telescope. A statistical analysis of the GRB data reveals that the events detected above 5σ are consistent with the thermal noise fluctuations.

Key words. Radio continuum: general — Gamma-ray burst: general — Methods: observational — Methods: data analysis

1. INTRODUCTION

Discovered by Lorimer et al. (2007), Fast Radio Bursts (FRBs) are characterized by extremely strong individual radio pulses of very short duration (in the order of millisecond) and with peak flux density reaching around several Jansky. In addition, FRBs are widely spread with dispersion measure DM, which is the integrated electron column density of free electrons along the line of sight, greater than the maximum Galactic value. Subsequent searches for FRBs in the last decade were conducted using the archival data from the Parkes 64-m (13-beam receiver) multibeam radio pulsar survey and from the Arecibo 300-m (7-beam receiver) radio telescope, which resulted in the discovery of another six FRBs (Thornton et al. 2013, Spitler et al. 2014). Recently, a great number of new FRBs were discovered in real-time search with Parkes telescope, CHIME and FAST, which also included measurements of their polarization properties (Bannister et al. 2017, Lorimer 2018, Bhandari et al. 2018, Caleb et al. 2017, Chatterjee et al. 2017). To date, over 800 unique sources have been published[1]. With wide field-of-view, repetitive coverage of the sky and good sensitivity, CHIME has discovered 24 repeating FRBs (CHIME/FRB Collaboration et al. 2019). Large samples of bursts have

[1] https://www.herta-experiment.org/frbstats/catalogue

also been recorded from some individual repeaters, which allows the study of their individual burst energy distributions and average spectra, as well as the change in their activity and properties with time. Li et al. (2021) found that the isotropic equivalent energy distribution of FRB 20121102A shows a multimodal distribution. This indicates that repeaters can produce multiple types of bursts, some of which appear arguably more similar to those seen from non-repeating FRBs. In addition, the recent detection of a bright FRB-like burst from the Galactic magnetar SGR 1935+2154 has provided an important link between FRBs and magnetars (Lin et al. 2020). FRBs, as one of the most tantalizing mysteries of our radio sky, have caused considerable discussion on their origins and potential use as cosmological tools. The large DMs associated with FRBs suggest that their progenitors could be extragalactic in origin. Currently, there are 19 FRBs that have been localized to their host galaxies[2]. Cordes and Wasserman (2016) examined the hypothesis that coherent processes in neutron star magnetospheres can produce such luminous bursts originating from extragalactic sources.

Gamma-ray Bursts (GRBs), as one class of the most powerful astronomical sources distributed isotropically and inhomogeneously in our universe, can be divided into short and long bursts based on the temporal and spectral properties (Kouveliotou et al. 1993). The extremely strong emission from GRBs are proposed to come either from high accretion of black holes (Lei et al. 2013) or millisecond pulsars with extremely strong magnetic fields (Usov 1992). According to the central engine model for millisecond pulsars, the rapidly rotating and highly magnetized neutron stars may emit strong radio pulses of short duration and at low frequency during the bursts, which could be detected by our radio telescopes (Usov and Katz 2000). Recently, Zhang (2014) proposed a magnetar model as the central engine for GRB. In this model, the supermassive neutron star undergoes rapid spin-down under its strong magnetic field before it collapses into a black hole as it loses the centrifugal support. The short strong radio burst will be emitted during the magnetar phase, which suggests that a small fraction of FRBs could be connected with GRBs. However, no GRB events are associated with FRBs, as none of the X-ray statellites are observing at the time and position of the FRBs. Thornton et al. (2013) and Spitler et al. (2014) ruled out the possibility that GRBs are the progenitors for most FRBs based on the inconsistency of the event rates. No counterpart from X-ray to radio wavelengths is identified, which ruled out the model for long-duration Gamma-ray burst and Galactic origin (Petroff 2014).

The verifications for the association of FRBs with GRBs have been provided by a variety of past and ongoing experiments that performed searches from a large range of frequencies for short duration radio pulses after γ-ray emission from GRBs. A search for coincident radio pulses from 19 GRB events at 151 MHz failed to locate any astronomical signals (Baird et al. 1975). This was due to the radio emission being significantly limited by propagation effects when they passed through the dense interstellar and/or intergalactic medium. Bannister et al. (2012) reported 9 GRB observations at 1.4 GHz using a 12-m radio telescope located at Parkes Observatory. They detected two dispersed short duration radio pulses with DM in excess of the expected Galactic electron-density contribution in the directions of GRBs, but later revealed that they were unlikely to be astrophysical by a joint analysis (Palaniswamy et al. 2014). In a motivated search for FRBs in association with five GRBs using a 26-m radio telescope equipped with rapid respond to GCN notifications at 2.3 GHz, a non-detection was reported at a sensitivity of 6σ for 3 Jy (Palaniswamy et al. 2014).

Also motivated by previous FRB searches, we aim to test the possible connection between GRBs and FRBs. Here, we report on the preliminary results of this search that no discovery of FRB bursts can be ssociated with the three GRBs with Signal-to-Noise Ratio (S/N) larger than 5. The structure of our paper is as follows. In Section 2, we describe our observations with the YNAO 40-m radio telescope at 2256 MHz. A detailed description of our single pulse search pipeline is also given. In Section 3, we present our results. We conclude the paper and summarize the results Section 4.

2. OBSERVATIONS AND DATA REDUCTION

We observed three GRBs listed in Table 1 with the 40-m radio telescope located at the YunNan Astronomical Observatory (YNAO) at a central frequency of 2256 MHz. The GRB notifications from the Gamma-ray Coordinates Network (GCN)[3] were received via email. Only the notices from the gamma-ray Burst Alert Telescope (BAT) on the *Swift* satellite with field-of-view of about $3'$ are filtered to be accepted. Once the accessible GRBs with elevation above 8° and within the visible range ($-45^\circ < \beta < +90^\circ$) of the radio telescope were identified, the coordinates of the GRBs was sent to the telescope control system. Then, the radio telescope would slew to the required position and began recording data.

The 40-m radio telescope has a Cassegrain optics and two orthogonal circular polarizations, which are split by an ortho-mode transducer (OMT) at the end of the horn feed. A S/X dual-channel room-temperature receiver is equipped to amplify and down-convert the signal to an analog intermediate frequency (IF) in the range of $(0 - 500)$ MHz using a local oscillator (LO) operating at 2256 MHz.

[2] https://frbhosts.org/

[3] www.gcn.gsfc.nasa.gov

Table 1: Details of the three GRBs observed with the 40-m radio telescope. α and β are the positions of a GRB in J2000.0 coordinates. $P_{\rm BAT}$ is the BAT position uncertainty. $T_{\rm BAT}$ is the time when the BAT detected a GRB. T_{90} is the duration of the GRB based on the BAT light curve. $T_{\rm rec}$ is the time when the recorders at YNAO 40-m radio telescope starts recording the signals from the source. $T_{\rm obs}$ is observational time duration for the source by the radio telescope. $T_{\rm ave}$ is the time resolution while recording the data.

Source	α (J2000.0)	β (J2000.0)	$P_{\rm BAT}$ (arcmin)	Trigger Date	$T_{\rm BAT}$ (UT)	T_{90} (s)	$T_{\rm rec}$ (UT)	$T_{\rm obs}$ (s)	$T_{\rm ave}$ (μs)
GRB140512A	$+19^{\rm h}17^{\rm m}29^{\rm s}$	$-15°06'$	3	2014 May 12	19:31:49	154.8	20:54:34	7200	1000
GRB140629A	$+16^{\rm h}35^{\rm m}56^{\rm s}$	$+41°53'$	3	2014 June 29	14:17:30	42.0	15:04:41	20510	100
GRB140703A	$+00^{\rm h}51^{\rm m}58^{\rm s}$	$+45°06'$	3	2014 July 03	00:37:17	67.1	01:15:45	10748	100

After that, the signals are fed to a filterbank system. The total bandwidth of the left and right circular polarized signals is 512 MHz from $(2000 - 2512)$ MHz. The analog IFs are divided into 1024 0.5-MHz sub-bands before digitization. The data are recorded for each subband in the standard pulsar data storage format of PSTFITS[4] with a time resolution of 1000 μs for GRB140512A and 100 μs for the other two GRBs, and a digitalization precision of 8-bit. The time stamp for the start of an observation is derived from a Global Positioning System (GPS). The recorded polarization products are in the format of 'AABBCRCI', where AA and BB are the direct products of the two A and B input channels, and CR and CI are the real and imaginary parts of the cross product from A*B. Bursts from some FRBs were reported to be highly linearly polarized with flat polarization angles across the bursts (Nimmo et al. 2021, Hilmarsson et al. 2021, Kumar et al. 2022). In subsequent data reduction, the two polarizations AA and BB are treated separately throughout the pipeline till the end of the processing.

For our experiment, the full width at half maximum for the primary beam of the radio telescope is about $30'$, which makes the observed GRBs fall in the beam. The pointing error of the 40-m radio telescope across the entire sky is $\sim 30''$. The System Equivalent Flux Density (SEFD) is measured to be ~ 280 Jy by using the system temperature of 76.93 K, the antenna efficiency of 60.22% and the diameter of a circular aperture antenna of 40 m. The limiting mean flux density for the 40-m radio telescope is calculated using the radiometer equation. Hence, the 5σ flux density sensitivity is calculated approximately equivalent to 2.5 Jy for time resolution of 1000 μs, and 8.0 Jy for 100 μs, with effective bandwidth of 150 MHz due to serious Radio Frequency Interference (RFI).

The recorded data were transferred to Xinjiang Astronomical Observatory (XAO) for off-line analysis. The data processing were performed using our single pulse search pipeline, which consists of RFI excision, DM search, event detection and classification of events.

[4]http://www.atnf.csiro.au/research/pulsar/index.html?n=Main.Psrfits

The first step in the pipeline is to identify and excise RFI from the terrestrial transmitters, radars, satellites, etc., which affects the total power as a function of frequency and time. The frequency bands contaminated by persistent RFI are identified and removed manually. For the short time samples with serious RFI across the whole frequency band, a thresholding method is used in the algorithm to remove the RFI. In this method, a range of time series is formed by summing over the frequency channels. The time samples that exceed a pre-set threshold of 3σ are excised and replaced with mean power value of the time series. The impulsive RFI was pre-dominantly observed due to high voltage power-line and automobile sparking, corona discharges and switching of inductive load. For the impulsive narrow-band RFI excision, the method described by Wen et al. (2021) was used. For each frequency channel, the interference deviates from the assumed Gaussian distribution of the noise. Bad channels with $S_f = \sum_t x_{t,f}^2/\mu^2$ greater than 12 standard deviation above the average are flagged and replaced by random values drawn from a Gaussian distribution with a mean of 1.0 and a standard deviation of 0.1, where $x_{t,f}/\mu$ is the sample at time t and frequency f after division by the average value (μ).

The astronomical impulsive radio signal will be dispersed when it passes through a cluster of ionized plasma in the interstellar and intergalactic medium. This causes the group velocity of the pulse at a higher frequency to be larger than that at a lower frequency. Consequently, the received radio pulses will be weaker and wider compared with the intrinsic signals. Therefore, the next step in our pipeline is to search for the real DM value by incoherent dedispersion for both polarizations. This is achieved through application of an appropriate time delay for each spectral channel and suming the power across all the spectral channels. The dedispersed time series of both polarizations are generated for DM ranging from 0 to 5000 pc/cm^3 with a step of 50 pc/cm^3. Each dedispersed time series is then searched for single pulse events above a defined signal-to-noise threshold. The finial step in the pipeline involves the classification of detected events $> 5\sigma$. The signatures of astronomical signals, low level RFI, and thermal noise fluctuations

are visually inspected and classified using the diagnostic plots.

3. RESULTS

The results of our search for FRBs associated with GRBs using the above detailed single pulse search pipeline are given in Table 2. The DM ranges from $0-5000$ pc/cm^3 with a step of 50 pc/cm^3. The number of events $> 5\sigma$ detected for all GRBs by our detector are listed in the second column. No signatures of astronomical signals from the three data sets are detected in the diagnostic plots via visual inspection. An example of diagnostic plot is shown in Fig. 1, which illustrates the distribution of the detected events $> 5\sigma$ for GRB140512A at 2256 MHz. The top panel presents the DM for all events with S/N $> 5\sigma$ plotted against time. The size of the circles are proportional to the S/N of the events. Palaniswamy et al. (2014) described the differences among the signatures of astronomical signals, low level RFI and thermal noise fluctuations in the DM-time plane. The astronomical signals are broadband, and expected to show a reduced S/N for DMs that deviates from the true DM. The recorded events that are $> 5\sigma$ from our detection pipeline for all observations do not show characteristic signature of an astronomical signal. Most of the events detected at a single DM step show S/N close to the detection threshold, and they are caused by thermal noise fluctuations. A small number of events appearing in multiple DM steps are caused by low level RFI, and so they do not possess the characteristic peaked shape similar to that of a bright pulse from an astronomical source.

In the absence of a characteristic signature of an astronomical signal $> 5\sigma$, a method similar to Bannister et al. (2012) is adopted for dealing with the number of false positives. In this method, the spectral channels are randomized before dedispersion using the data from the GRB observations. The properties of thermal noise fluctuations and low level RFI will be perserved for statistical analysis. The third column in Table 2 shows the number of false positive events above 5σ, which is less than the detected candidates. The method of randomizing the frequency channels destroys the dispersion relation of $t \propto f^{-2}$ expected from astronomical signals, and preserves the thermal noise fluctuations, narrow and wide band RFI, while the impulsive RFI with intermediate bandwidth are also destroyed. Additionally, the amount of background detections are reduced as well. The effect of impulsive RFI is estimated to be $> 20\%$ in comparison with other RFIs.

4. DISCUSSION AND CONCLUSIONS

Our experiment is designed to be very similar to the previous ones. The statistical analysis of the detected events by randomizing the spectral channels using the data from GRB observations shows that the number of false positives due to thermal noise fluctuations and RFI is less than the number of candidates. The reduced number of false positives is due to preservation of the properties of thermal noise fluctuations, narrow and wide band RFI while the impulsive RFI spanning over multiple frequency channels are destroyed.

Following the statistical analysis of detection described by Palaniswamy et al. (2014), the probability for detecting events $> S_{\rm min}$ is given by:

$$P(S > S_{\rm min,B12}) = (\frac{S_{\rm min,B12}}{S_0})^{-\alpha_{\rm r}+1}, \qquad (1)$$

where $\alpha_{\rm r} = 2.5$, $S_0 = 0.189$Jy is the low flux density cutoff. The flux density as a function of spectral index is described by a power-law:

$$S_{\rm min,B12} = \alpha_{\rm B12}\sigma_{\rm B12}(\frac{\nu_{\rm W15}}{\nu_{\rm B12}})^{\beta_{\rm r}}, \qquad (2)$$

where α is the S/N ratio threshold for detecting an event, σ is the sensitivity of the telescope at time resolution of 25 ms, and ν is the observing frequency. Thus, the joint probability distributions for low and high frequencies are derived, which are depicted in dashed and dash-dotted lines in Fig. 2, respectively. The solid line describes the total probability for the results of Bannister et al. (2012) and ours. Two cases of two and one events detected by Bannister et al. (2012) are presented in the top and bottom panels of Fig. 2. The parameters of the other GRB experiments are obtained from the references in Palaniswamy et al. (2014). The probability for detecting one event is larger than that for detecting two events. Our results are consistent with Palaniswamy et al. (2014) in that two FRBs from GRBs are unlikely to be astrophysical. Furthermore, the FRBs with spectral index $\beta_r < -2$ are easier to be detected at low frequencies, while the FRBs with spectral index $\beta_r > -0.5$ are easier to be detected at high frequencies. The radio spectral indices for the events are constrained to be $-2 < \beta_r < -0.5$ under the condition that the events detected by Bannister et al. (2012) are real.

The simplest conclusion is that no FRB in association with the three GRBs is detected at the sensitivity of the YNAO 40-m radio telescope. The conservative upper limits for the radio flux density measured at Earth are estimated to be 2.5 Jy for GRB140512A with time resolution of 1 ms and 8.0 Jy for GRBs 140629A and 140703A with sampling time of 0.1 ms, taking into account the various antenna system currently in use.

The absence of characteristic signatures of an astronomical signal $> 5\sigma$, can be argued as follows.

(1) The radiated short duration radio pulses may be absorbed by the GRB blast wave in front of the emission region (Zhang 2014).

(2) The FRBs are proposed to be produced when a spinning supermassive neutron star loses the centrifugal support and collapses into a black

Table 2: A summary of the statistical analysis performed on all the GRB data sets. From left to right, the columns are: the source name, the actual number of events detected above 5σ, the expected number of events above 5σ due to thermal noise fluctuations, the sensitivity of the telescope.

GRB Name	$N_A(I > 5\sigma)$	$N_E(I > 5\sigma)$	Sensitivity (Jy)
GRB120512A	1581566	1263286	2.5
GRB140629A	8106047	5298069	8.0
GRB140703A	4043891	2909274	8.0

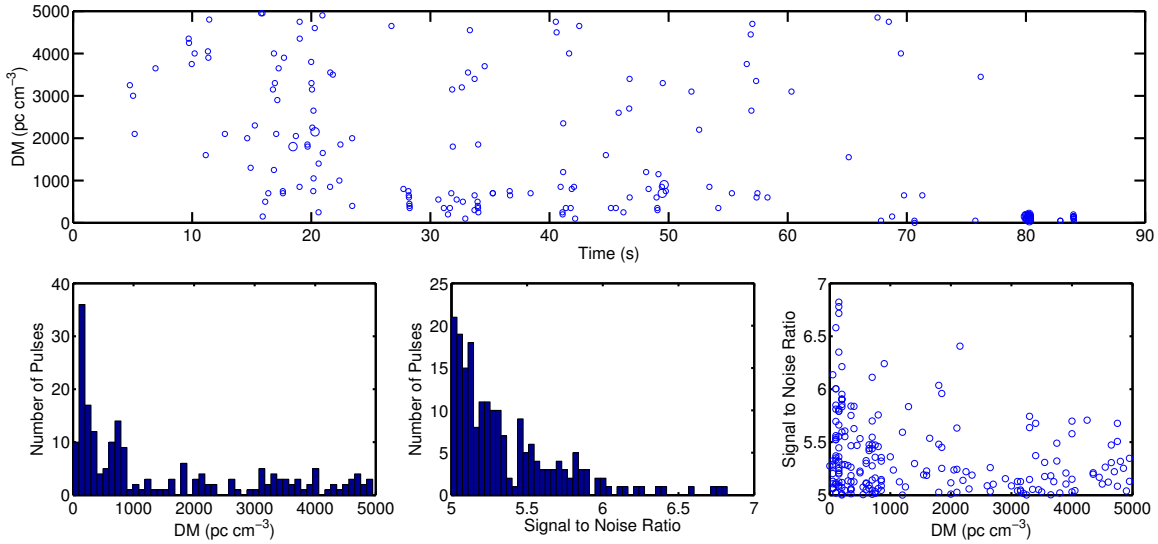

Fig. 1: Example diagnositc plot that illustrates the distribution of detected events $> 5\sigma$ for GRB140512A at 2256 MHz. Top panel: The DM values for all events with S/N $> 5\sigma$ plotted against time. The size of circles are proportional to the S/N of the events. Lower left panel: distribution of the DM for detected events. Lower middle panel: distribution of the S/N for detected events. Lower right panel: scatter plot of the DM and S/N. No signatures of astronomical signal are detected with S/N $> 5\sigma$.

hole. The implosions can happen in supermassive neutron stars shortly after their births from hundreds to thousands of seconds. Within the framework, some GRBs may have generated an FRB $10^2 - 10^4$ s after the GRB trigger. The radio bursts are out the period of our observations as the time separation between radio and γ-ray emission are unlikely too large, the arrival times of the radio pulses should coincide with the breaks in the GRBs X-ray light curves (Zhang 2014).

(3) The flux densities of the FRBs during our observations are below the sensitivity of our radio telescope, which is similar to the non-detection of radio pulses in previous surveys (Koranyi et al. 1995, Dessenne et al. 1996, Katz et al. 2003).

(4) Recently, Cordes & Wasserman argued that the FRBs could originate from extragalactic neutron stars, which have no physical association with GRBs.

(5) The spectral indices are flatter with values larger than -0.5, which are easier detected at higher frequencies.

(6) Only a fraction of GRBs emit radio pulses (Zhang 2014). Most FRBs are not supposed to be associated with GRBs, because not all GRBs originate from supermassive millisecond magnetars as the central engine.

Acknowledgements – We would like to thank the anonymous referee for providing constructive suggestions to improve the article. We thank the staff of the YNAO 40 meter radio telescope group who have made these observations possible. This work is partially supported by the National Key Research and Development Program of China (No. 2022YFC2205203), the Major Science and Technology Program of Xinjiang Uygur Autonomous Region (No. 2022A03013-1), the National Natural Science Foundation of China (NSFC grant No. 11988101, U1838109, 12041304, 12203094, 12041303, 12041301, 11873080, 12133004 and U1631106), the National SKA Program of China (2020SKA0120100, 2020SKA0120200), the Chinese Academy of Sciences Foundation of the young scholars of western (No. 2020-XBQNXZ-019), and Xinjiang Key Laboratory

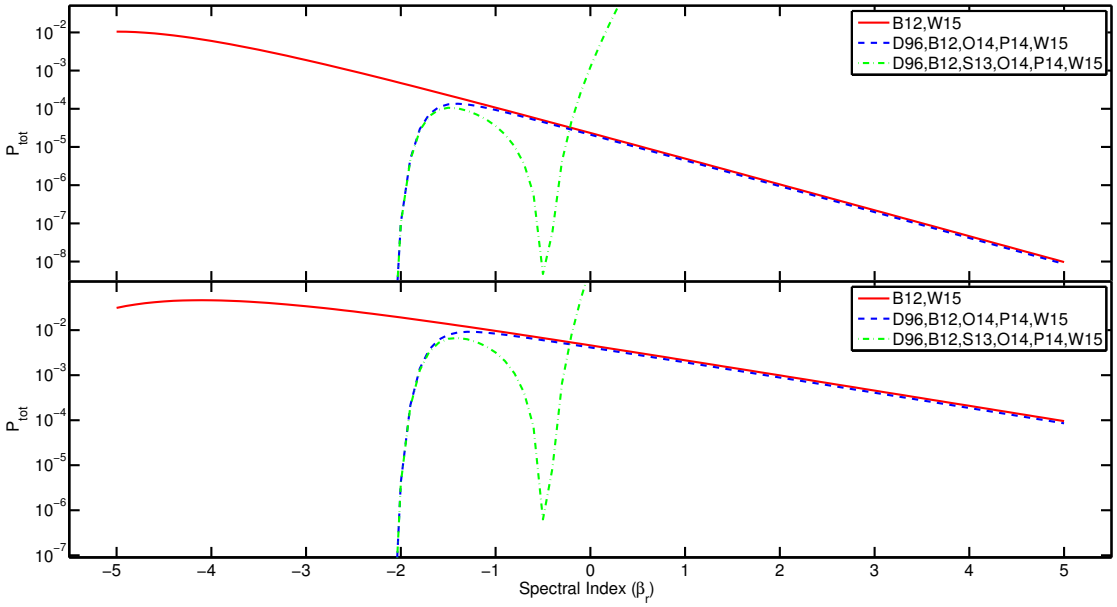

Fig. 2: Top panel: the joint probability as a function of spectral index,β_r, for detecting B12 with two events and zero event in the other experiments. Bottom panel: the joint probability as a function of spectral index, β_r, for detecting B12 with one real event and zero event in the other experiments.

of Radio Astrophysics (No. 2022D04058). ZGW is supported by the 2021 project Xinjiang Uygur autonomous region of China for Tianshan elites and the Youth Innovation Promotion Association of CAS under No. 2023069. RY is supported by the Key Laboratory of Xinjiang Uygur Autonomous Region (No. 2020D04049).

REFERENCES

Baird, G. A., Delaney, T. J., Lawless, B. G., et al. 1975, ApJL, 196, L11
Bannister, K. W., Murphy, T., Gaensler, B. M. and Reynolds, J. E. 2012, ApJ, 757, 38
Bannister, K. W., Shannon, R. M., Macquart, J. -P., et al. 2017, ApJL, 841, L12
Bhandari, S., Keane, E. F., Barr, E. D., et al. 2018, MNRAS, 475, 1427
Caleb, M., Flynn, C., Bailes, M., et al. 2017, MNRAS, 468, 3746
Chatterjee, S., Law, C. J., Wharton, R. S., et al. 2017, Natur, 541, 58
CHIME/FRB Collaboration, Andersen, B. C., Bandura, K., et al. 2019, ApJL, 885, L24
Cordes, J. M. and Wasserman, I. 2016, MNRAS, 457, 232
Dessenne, C. A. -C., Green, D. A., Warner, P. J., et al. 1996, MNRAS, 281, 977
Hilmarsson, G. H., Spitler, L. G., Main, R. A. and Li, D. Z. 2021, MNRAS, 508, 5354
Katz, C. A., Hewitt, J. N., Corey, B. E. and Moore, C. B. 2003, PASP, 115, 675
Koranyi, D. M., Green, D. A., Warner, P. J., Waldram, E. M. and Palmer, D. M. 1995, MNRAS, 276, L13
Kouveliotou, C., Meegan, C. A., Fishman, G. J., et al. 1993, ApJL, 413, L101
Kumar, P., Shannon, R. M., Lower, M. E., et al. 2022, MNRAS, 512, 3400
Lei, W.-H., Zhang, B. and Liang, E.-W. 2013, ApJ, 765, 125
Li, D., Wang, P., Zhu, W. W., et al. 2021, Natur, 598, 267
Lin, L., Zhang, C. F., Wang, P., et al. 2020, Natur, 587, 63
Lorimer, D. R. 2018, NatAs, 2, 860
Lorimer, D. R., Bailes, M., McLaughlin, M. A., Narkevic, D. J. and Crawford, F. 2007, Sci, 318, 777
Nimmo, K., Hessels, J. W. T., Keimpema, A., et al. 2021, NatAs, 5, 594
Palaniswamy, D., Wayth, R. B., Trott, C. M., et al. 2014, ApJ, 790, 63
Petroff, E. 2014, X-ray follow-up of a fast radio burst, Chandra proposal ID #16408500
Spitler, L. G., Cordes, J. M., Hessels, J. W. T., et al. 2014, ApJ, 790, 101
Thornton, D., Stappers, B., Bailes, M., et al. 2013, Sci, 341, 53
Usov, V. V. 1992, Natur, 357, 472
Usov, V. V. and Katz, J. I. 2000, A&A, 364, 655
Wen, Z. G., Yuen, R., Wang, N., et al. 2021, ApJ, 918, 57
Zhang, B. 2014, ApJL, 780, L21

ПРЕТРАГА ЗА БРЗИМ РАДИО-БЉЕСКОВИМА АСОЦИРАНИМ СА ГАМА БЉЕСКОВИМА КОРИШЋЕЊЕМ 40-МЕТАРСКОГ РАДИО-ТЕЛЕСКОПА НА АСТРОНОМСКОЈ ОПСЕРВАТОРИЈИ ЈУНАН

Y. F. Zhang[1,2], Z. G. Wen[2], N. Wang[2], L. F. Hao[3], J. P. Yuan[2], R. Yuen[2], X. F. Duan[2,4], and Z. Wang[1,2]

[1] *School of Physical Science and Technology, Xinjiang University, Urumqi, Xinjiang, 830046, People's Republic of China*

[2] *Xinjiang Astronomical Observatory, Chinese Academy of Sciences, 150, Science-1 Street, Urumqi, Xinjiang, 830011, People's Republic of China*

[3] *Yunnan Astronomical Observatory, Chinese Academy of Sciences, Kunming, 650011, People's Republic of China*

[4] *Xinjiang Key Laboratory of Microwave Technology, Urumqi, Xinjiang, 830011, People's Republic of China*

E–mail: *wenzhigang@xao.ac.cn*

УДК 52–121 + 52–732 + 52–77
Претходно саопштење

Извештавамо о резултатима претраге брзих радио-бљескова (Fast Radio Bursts, FRB) из три гама бљеска (Gamma-ray bursts, GRB) на 2256 MHz користећи 40-метарски радио-телескоп на Астрономској опсерваторији Јунан (YAO). Потрага за сигналима иницирана је детекцијама инструмента BAT (Burst Alert Telescope), који се налази на сателиту Swift. Појединачни радио-импулси су тражени у подацима преко великог опсега мере дисперзије, од 0 до 5000 pc/cm^3, са кораком од 50 pc/cm^3. Емисије сличне брзим радио-бљесковима нису забележене у иницијалној фази гама-бљескова са значајношћу већом од 5 σ. Ако постоје брзи радио-бљескови повезани са гама-бљесковима, постављамо горњу границу густине флукса радио-импулса од 2.5 Jy за GRB140512A i 8.0 Jy за GRB 140629A и 140703A, користећи осетљивост телескопа. Статистичка анализа података о гама-бљесковима показује да су догађаји детектовани изнад 5 σ у складу са флуктуацијама термалног шума.